33rd Annual International Conference of the IEEE EMBS
Boston, Massachusetts USA, August 30 - September 3, 2011

High-frequency limit of neural stimulation with ChR2

N. Grossman, K. Nikolic, M. S. Grubb, J. Burrone, C. Toumazou, Fellow, IEEE, P. Degenaar

Abstract— Optogenetic technology based on light activation of genetically targeted single component opsins such as Channelrhodopsin-2 (ChR2) has been changing the way neuroscience research is conducted. This technology is becoming increasingly important for neural engineering as well. The efficiency of neural stimulation with ChR2 drops at high frequencies, often before the natural limit of the neuron is reached. This study aims to investigate the underlying mechanisms that limit the efficiency of the stimulation at high frequencies. The study analyzes the dynamics of the spikes induced by ChR2 in comparison to control stimulations using patch clamp current injection. It shows that the stimulation dynamics is limited by two mechanisms: 1) a frequency independent reduction in the conductance-to-irradiance yield due to the ChR2 light adaptation process and 2) a frequency dependent reduction in the conductance-to-current yield due to a decrease in membrane re-polarization level between spikes that weakens the ionic driving force. The effect of the first mechanism can be minimized by using ChR2 mutants with lower irradiance threshold. In contrast the effect of the second mechanism is fundamentally limited by the rate the native ion channels re-polarize the membrane potential.

I. Introduction

OPTOGENETICS technology that combines optics and genetics has been revolutionizing the way researchers interface with neurons [1]. Using genetically encoded agents such as Channelrhodopsin-2 (ChR2) [2], light sensitivity can be imparted onto otherwise 'blind' neuronal cells. The cells can then be optically activated using remote light sources. Since its introduction to neuroscience [3], ChR2 has been used extensively in in-vitro and in-vivo research [4], and it has been investigated for clinical applications such as retinal prosthesis [5-6] and other aspects of neurotechnology [7]. Stimulating neurons with ChR2 is however fundamentally different from the traditional electrical approaches.

ChR2 is a cation channel from the green algae Chlamydomonas reinharditii, see e.g. [8-9]. In nature, ChR2 helps the algae to take a position in optimal photosynthesis conditions. Like other opsin-based proteins, ChR2 absorbs light through its interaction with retinal which undergoes a trans–cis isomerization. The retinal isomerization induces a series of conformation changes in the protein that can eventually lead to the opening of an ion conducting pore. When ChR2 is expressed in the neuron's membrane, opening of the pore practically increases the membrane's conductance which leads to cytoplasmic current.

ChR2 is a passive conductor and not a current source and it exhibits nonlinear characteristics [10] that affect the dynamics and fidelity of the elicited action potentials. The temporal resolution of ChR2 stimulation does not always match the one that is achieved by the electrical stimulation. The fidelity of ChR2 based stimulation drops at high frequencies, often before the natural limit of the neuron is reached, for example: Boyden et al. 30Hz [3], Li et al. 5Hz [11], Ishizuka et al. 20Hz [12], Arenkiel et al. and Wang et al. 40Hz [13]. This drop in efficiency at high frequencies led to efforts to develop fast mutants of ChR2: ChETA [14], ChD [15] and CatCh [16] (though mutating ChR2 can compromise other important properties of ChR2 [17]). A detailed study of the potential effect of these mutations on the spiking output was recently described by us [18].

The aim of this study is to investigate the underlying mechanisms that limit the temporal resolution of ChR2 stimulation in order to help researchers to interpret experimental results, design illumination protocols and develop strategies for interfacing with neural tissue.

II. Methodology

The methodology of this study is based on a comparison between a ChR2-based stimulation and a controlled current injection using a patch clamp technique.

A. Cell culture and transfection

The study uses rat hippocampal neurons that were transfected with a fusion protein ChR2-YFP. The ChR2-YFP vector was subcloned into a plasmid containing a chick β-actin promoter. Primary dissociated cultures were obtained from rat hippocampal tissue on embryonic day 18.5. Hippocampi were digested in trypsin (1 mg/ml in HBSS, 15 min at 37 ^{o}C), and dissociated in neurobasal medium with 10% FCS by passing through a series of decreasing diameter Pasteur pipettes. They were then plated at 300 cells/mm^2 on 18mm diameter glass cover-slips coated in PDL (50 μg/ml) and laminin (20 μg/ml). Neurons were transfected with the appropriate ChR2 vector using a lipofectamine procedure at 7 days in vitro (DIV).

B. Optical Stimulation

The cell were illuminated with a fast shuttering (<1ms 10% to 90%), directly modulated diode pumped solid state (DPSS) 473 nm laser (DPBL-9020, Sp3 plus). The on-sample illumination and laser shuttering kinetics were characterized prior to the stimulation experiments. The laser

N. G., K. N. and C.T. are with the Institute of Biomedical Engineering, Department of Electrical and Electronic Engineering, Imperial College London, SW7 2AZ, UK.; ({nir.grossman,k.nikolic} @ imperial.ac.uk).

P. D. is with the Department of Electrical Engineering, Newcastle University, UK.

M. S. G. and J. B. are with the Department of Developmental Neurobiology, King's College, London, UK.

was focused using a single lens to a 125 µm full wave half maximum (FWHM) spot diameter. The spot size was measured from a fluorescent image of the matrix on a thin fluorescent sheet. The illumination beam was focused on the somas of the neurons to allow for a fair comparison with the somatic injection stimulations. The images were taken with a CCD camera (Orca ER) and analyzed with Origin 8.0 (OriginLabs). We used 40mW/mm^2 saturating irradiance to minimize potential errors due to small fluctuation in the laser output. The on-sample power was measured by imaging the emitter on the FieldMaxII-TO (Coherent) power meter that was placed in the image plane.

C. Electrophysiology

Electrophysiological recordings were performed at ≥ 10 DIV using patch clamp method. Individual coverslips were placed in a custom recording chamber and bathed with room-temperature HEPES-buffered saline (HBS) containing, in mM: 136 NaCl, 2.5 KCl, 10 HEPES, 10 D-glucose, 2 CaCl2, 1.3 MgCl2, 0.01 gabazine, 0.01 NBQX, and 0.025 APV (285mOsm, pH7.4). Patch pipettes, pulled from borosilicate glass (1.5mm OD, 1mm ID, 3-4 M) were filled with a solution containing, in mM: 130 K-gluconate or Cs-gluconate, 10 NaCl, 1 EGTA, 0.133 CaCl2, 2 MgCl2, 10 HEPES, 3.5 Na-ATP, 1 Na-GTP (280mOsm, pH7.4). Conventional whole-cell patch-clamp recordings were obtained via a Heka EPC10 double patch amplifier coupled to Pulse acquisition software. Signals were sampled at intervals of 65-150 µs (6.7-15.4 kHz) and were low-pass filtered using a 4-pole Bessel filter at 2.9 kHz (filter 2). Electrical stimulation was achieved by injecting currents that were tuned to produce the same steady state spiking frequencies as ChR2 in a constant stimulation mode.

D. Data Analysis

All numerical calculations were performed in MATLAB 7.5.0 (The Mathworks, Natick, MA). When analyzing the action potentials we considered only depolarization spikes that exceeded 0mV to be valid. The rate of change in the membrane potential (dV_m/dt) was calculated and the maximum depolarization and repolarization rates were identified. The spiking threshold was defined as the voltage at the onset of each spike at which dV_m/dt reached approximately 5% of its maximum value. ChR2 photocurrents were estimated by recording the neural responses under both current and voltage clamp conditions. First, the instantaneous ChR2 conductance was calculated from the voltage clamp measurements ($G_{ChR2}(t)=I(t)/V_{clamp}$). Then, the photocurrents were calculated by multiplying the instantaneous conductance by the recorded (at current clamp conditions) membrane potential.

III. Results & Discussion

Fig. 1 shows an exemplary spike train at the resolution limit of ChR2. The left panel presents the spiking output from a constant current injection of 200pA (bottom) and a constant illumination of 40mW/mm^2 light (top). The magnitude of the stimulations was tuned to produce the same steady state spiking frequencies of ~33Hz. Using the same current and irradiance amplitudes, the stimulations were then switched to a pulse mode. For frequencies up to 40Hz both generated stable spiking. From ~50Hz, the fidelity of light stimulation started to drop, while current stimulation stayed reliable at frequencies >70Hz. Fig.1 (right) shows recordings for 50Hz and 10ms pulse width. The current injection stimulation elicited a complete spike train with stable ~2.5ms spike latencies. In contrast, the ChR2 based stimulation elicited an incomplete spike train, with spike latencies that constantly increased. A more detailed analysis of these stimulation patterns is shown in Fig 2.

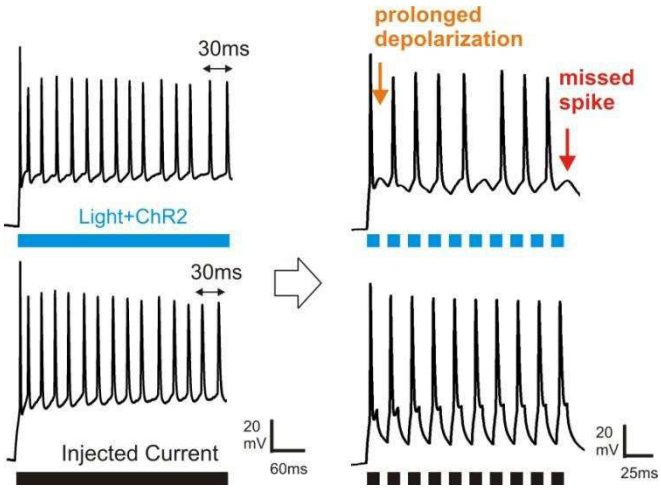

Fig. 1. Plot shows patch clamp recording from ChR2 (top blue) and current injection (bottom black) stimulation. Under constant stimulation (left) both methods induced the same steady state frequency however when they were switched to 50Hz pulse mode (right), ChR2 elicited spikes with longer post-spike depolarization and lower fidelity. Light irradiance: 40mW/mm^2; current injection: 200pA; pulse width: 10ms.

In principle, an increase in the spiking latencies can happen during the natural frequency adaptation process of the neuron [19]. The neural adaptation mechanism is based on modulation of the spiking threshold, which is typically associated with an incomplete re-polarization of the membrane potential between spikes that reduces the recovery of the voltage gated Na^+ channels and/or maintains a sub-threshold K^+ conductance. Fig. 2a shows that this mechanism was however not activated in the example given. Here, the spiking threshold during ChR2 stimulation was in fact (~10mV) lower than electrical stimulation, although the re-polarization of the membrane potential was slightly (5-10%) weaker with ChR2. The increase in the spike latencies was therefore related to ChR2 mechanisms and not to the neuron ones. Fig. 2(c) shows that at lower frequencies ChR2 stimulation was able to elicit a stable spike patterns.

In order to reveal the mechanisms that prolong the spike latencies, we compared in Fig. 3 a steady (or "stable") 10Hz ChR2 stimulation with an "unstable" 50Hz ChR2 stimulation. Fig. 3(a) (left panel) shows the rate by which the ChR2 currents depolarized the membrane at the initiation of the elicited spikes. At the first spike, the depolarization rates are obviously the same. In the example given, ChR2 currents had maximal rate of 25mV/ms at this stage, which

resulted in a spike latency of ~2ms (note that at this pulse, ChR2 stimulation is slightly stronger than the corresponding current injection one). At the initiation of the third action potential however, the depolarization rate of the two stimuli differ considerably. The rate of depolarization dropped by 10mV/ms (~40%), during 10Hz stimulation and by 20mV/ms (80%) during 50Hz stimulation. After the third spike the depolarization rate remained stable in both cases.

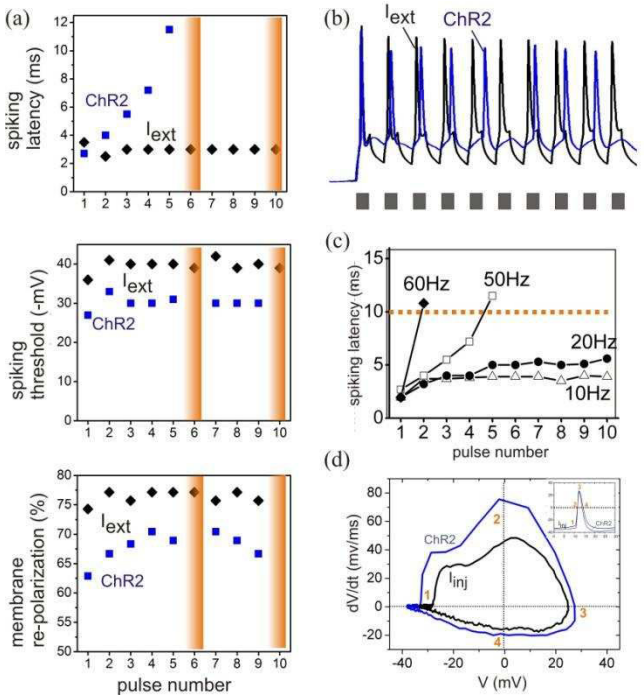

Fig. 2. ChR2 vs. current injection at 50Hz stimulation. (a) Spike latency (top); normalized to rest potential -65mV and spiking threshold (middle) calculated as V(threshold) – V(rest); maximum inter-spike membrane re-polarization (bottom). (b) An overlaid plot of the 50Hz light pulses of 40 mW/mm^2 (blue) and direct 200pA current injection (black) shown in Fig 1 (right). (c) Spike latencies profile for various illumination frequencies. (d) Phase plot diagram of steady-state spike from Fig 1 (right). ChR2 (blue). Current injection (black); Pointers 1-4 correspond to spike threshold, maximum spike rising rate, spike peak and maximum spike re-polarization rate, respectively.

The drop in the depolarization efficiency during the 10Hz stimulation is related to the intrinsic adaptation process in ChR2 conductance, see Fig 3b (left panel). The adaptation process is the result of ChR2 intrinsic photocycle [2, 20]. The level of adaptation is determined by the light irradiance, and it does not depend on the pulsing frequency, as shown in Fig 3b. The duration of the pulses can affect the rate by which the process reaches the steady state conductance.

Thus, both 10Hz and 50Hz illuminations induced the same membrane conductances but the resulted currents were very different, Fig. 3b (right panel). The current that was generated during the 50Hz illumination was almost 50pA smaller than the one generated at 10Hz illumination. The additional reduction in ChR2 currents at 50Hz is caused by a different mechanism. This mechanism is related to the fact that ChR2 is a passive conductor and not a current source. This means that the level of the membrane potential between the spikes can affect the magnitude of ChR2 currents.

Fig. 3(a) (right panel) shows that the membrane potential re-polarized back to its rest value during 10Hz illumination, thus maintaining a constant driving force at the initiation of the spikes. In contrast, the membrane potential remained almost 15mV depolarized during the 50Hz illumination, which reduces the driving force by almost a third. The incomplete re-polarization of the membrane potential weakened the force that drives the ions across ChR2 pores.

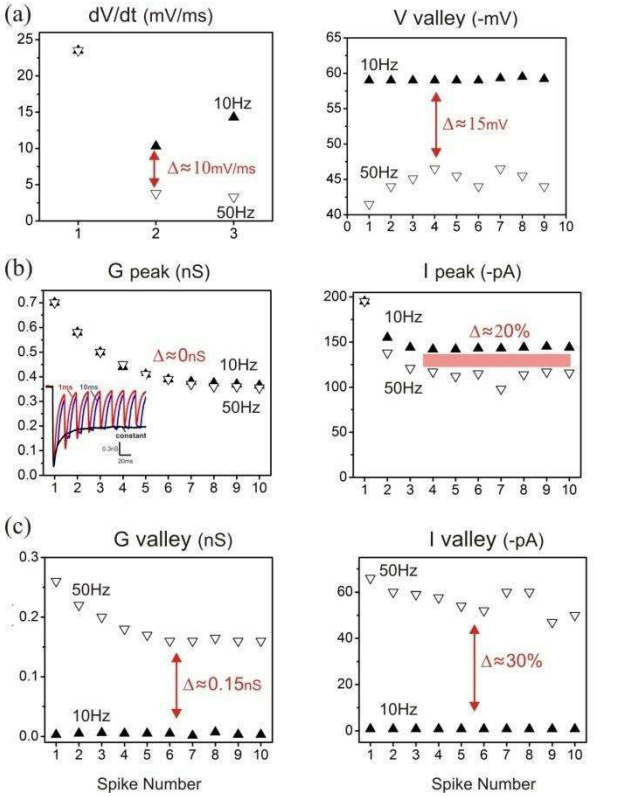

Fig. 3. Stable 10Hz vs. unstable 50Hz ChR2 stimulation. (a) Membrane depolarization rate at the initiation of the first three spikes (left). Minimum inter-spike membrane potential (right, note negative values). (b) ChR2 peak conductance (left). Inset: conductance traces measured by clamping the voltage to the rest potential (-65mV). ChR2 peak currents (right). (c) Minimum inter-spike ChR2 conductance (left). Minimum inter-spike ChR2 current (right). Full symbol 10 Hz, empty symbol 50 Hz.

The rate of membrane re-polarization is fundamentally governed by the native ion channels [19]. However, residual ChR2 conductance between spikes can generate dark photocurrents that resist the re-polarization process, as shown in Fig. 3(c). The limiting mechanism here is the shuttering speed of ChR2. During 50Hz stimulation only 63% of the opened ChR2s were closed between pulses (compare to 99% in the case of 10Hz), which left 150-250pS conductance, generating more than 50pA of depolarizing currents in the dark periods. In comparison there was ~0pA between spikes at 10Hz.

In constant stimulation mode, the passive conductance of ChR2 had some advantages. Fig. 2 shows that the steady-state spikes that were induced by ChR2 show smaller inter-spike re-polarization, lower spiking threshold, stronger depolarization rate after the spikes were triggered, stronger re-polarization rate after the spike peak, and slightly

narrower spikes width. At constant stimulation conditions, the passive conductance of ChR2 introduces smaller resistance once the spikes are triggered, which helps to maintain strong re-polarization. A strong re-polarization process can help the recovery of the Na^+ channels and minimize the accumulation of sub-threshold K^+ channels. In engineering terms, it implies that the feedback mechanism between ChR2 and the neuron ensures good recovery of the neural system from its action potential oscillations.

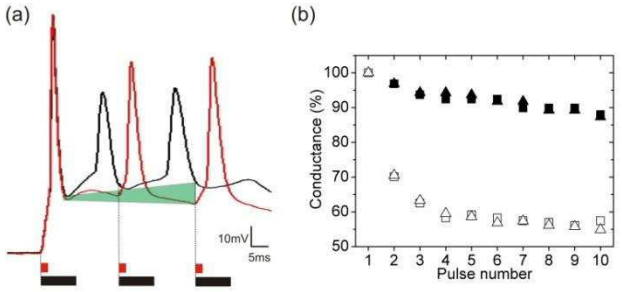

Fig. 4. Improvement strategies. (a) 50Hz ChR2 stimulation using 1ms (red) and 10ms (black), 40mW/mm^2. Differences in membrane re-polarization are highlighted in green.(b) Relative ChR2 peak conductance during 40mW/mm2 (full symbols) and 1mW/mm2 (empty symbols); 10Hz rectangular, 50Hz triangle.

IV. CONCLUSIONS

The process of stimulating action potentials with ChR2 is different from the traditional electrical approaches by: 1) intrinsic adaptation process, 2) sensitivity to membrane depolarization (negative feedback) and 3) slower closing kinetics. These principal differences result in unique spiking characteristics. This study investigated the effect of these differences on a specific neuron cell type at somatic illumination conditions, but the underlying principles it revealed are applicable to a wide range of neurons and experimental conditions. The strength of ChR2 stimulation declines along the stimulation process due to the protein intrinsic adaptation. This frequency-insensitive mechanism can reduce the conductance/irradiance yield by up to 50%. The effect of this mechanism can be minimized by reducing the threshold irradiance [18], or by producing a more stable ChR2 mutation [15] (though this often compromises the shuttering speed). Very recently, a new mutant ChR2 with marked improvement in channel kinetics while preserving photocurrent amplitudes was reported [21].

The strength of ChR2 stimulation can further decline at high frequencies due to incomplete re-polarization of the membrane potential, which decreases the ionic driving force across the membrane. The effect of this mechanism increases with frequency- higher stimulation frequency have shorter inter-spike periods which reduce the membrane re-polarization. This mechanism can be minimized by delivering the optical stimulation in short and intense pulses [18] see Fig. 4, or by producing a faster ChR2 [14-16]. However, the strength of ChR2 stimulation in pulse mode is always limited by the rate by which the neuron native ion channels restore the rest membrane potential.

ACKNOWLEDGMENT

This work was funded by the UK Biological and Biotechnology Research Council (F021127), the UK Engineering Physical Sciences Research Council (F029241 and H024581) and the University of London Central Research. The authors would like to express their gratitude to Karl Deisseroth for the ChR2 vector.

REFERENCES

[1] K. Deisseroth, "Optogenetics," Nature Methods, vol. 8, pp. 26-9, 2010.

[2] G. Nagel, et al., "Channelrhodopsin-2, a directly light-gated cation-selective membrane channel," Proc Natl Acad Sci U S A, vol. 100, pp. 13940-5, Nov 25 2003.

[3] E. S. Boyden, et al., "Millisecond-timescale, genetically targeted optical control of neural activity," Nature Neurosci, vol. 8, pp. 1263-8, Sep 2005.

[4] S. C. Rogan and B. L. Roth, "Remote Control of Neuronal Signaling," Pharmacol Rev, Mar 17.

[5] P. S. Lagali, et al., "Light-activated channels targeted to ON bipolar cells restore visual function in retinal degeneration," Nature Neurosci, vol. 11, pp. 667-75, Jun 2008.

[6] P. Degenaar, et al., "Optobionic vision--a new genetically enhanced light on retinal prosthesis," J Neural Eng, vol. 6, p. 035007, Jun 2009.

[7] N. Grossman, et al., "Multi-site optical excitation using ChR2 and micro-LED array," J Neural Eng, vol. 7, p. 16004, Feb 2010.

[8] P. Hegemann, "Algal sensory photoreceptors," Annu Rev Plant Biol, vol. 59, pp. 167-89, 2008.

[9] C. Bamann, et al., "Microbial rhodopsins in the spotlight," Curr Opin Neurobiol, vol. 20, pp. 610-6, Oct 2010.

[10] K. Nikolic, et al., "Modeling and engineering aspects of channelrhodopsin2 system for neural photostimulation," Conf Proc IEEE Eng Med Biol Soc, vol. 1, pp. 1626-9, 2006.

[11] X. Li, et al., "Fast noninvasive activation and inhibition of neural and network activity by vertebrate rhodopsin and green algae channelrhodopsin," Proc Natl Acad Sci U S A, vol. 102, pp. 17816-21, Dec 6 2005.

[12] T. Ishizuka, et al., "Kinetic evaluation of photosensitivity in genetically engineered neurons expressing green algae light-gated channels," Neurosci Res, vol. 54, pp. 85-94, Feb 2006.

[13] B. R. Arenkiel, et al., "In vivo light-induced activation of neural circuitry in transgenic mice expressing channelrhodopsin-2," Neuron, vol. 54, pp. 205-18, Apr 19 2007.

[14] L. A. Gunaydin, et al., "Ultrafast optogenetic control," Nature Neurosci, vol. 13, pp. 387-92, Mar 2010.

[15] J. Y. Lin, et al., "Characterization of engineered channelrhodopsin variants with improved properties and kinetics," Biophys J, vol. 96, pp. 1803-14, Mar 4 2009.

[16] S. Kleinlogel, et al., "Ultra light-sensitive and fast neuronal activation with the Ca(2+)-permeable channelrhodopsin CatCh," Nature Neurosci, Mar 13 2011.

[17] J. Y. Lin, "A user's guide to channelrhodopsin variants: features, limitations and future developments," Exp Physiol, vol. 96, pp. 19-25, Jan 2010.

[18] N. Grossman, et al., "Modeling Study of the Light Stimulation of a Neuron Cell with Channelrhodopsin-2 Mutants," IEEE Trans Biomed Eng, Feb 14 2011.

[19] B. P. Bean, "The action potential in mammalian central neurons," Nat Rev Neurosci, vol. 8, pp. 451-65, Jun 2007.

[20] K. Nikolic, et al., "Photocycles of Channelrhodopsin-2," Photochemistry and Photobiology, vol. 85, pp. 400-411, 2009.

[21] A. Berndt, et al., "High-efficiency channelrhodopsins for fast neuronal stimulation at low light levels," Proc Natl Acad Sci U S A, vol. 108, pp. 7595-7600, 2011.